Removal of Basic Fuchsin Red dye by Turmeric leaf waste biochar: Batch adsorption studies, isotherm kinetics and RSM studies

[1]Nithyalakshmi B* [2]Saraswathi R and [3]Praveen S

[1]Department of Civil Engineering, Kumaraguru College of Technology, Coimbatore, India

[2]Department of Civil Engineering, Coimbatore Institute of Technology, Coimbatore, India

[3]ECOSTP Technologies Private Limited, Bengaluru, India

*Author for correspondence: nithyalakshmi.b.ce@kct.ac.in; nithyalakshmiprem@gmail.com

GRAPHICAL ABSTRACT

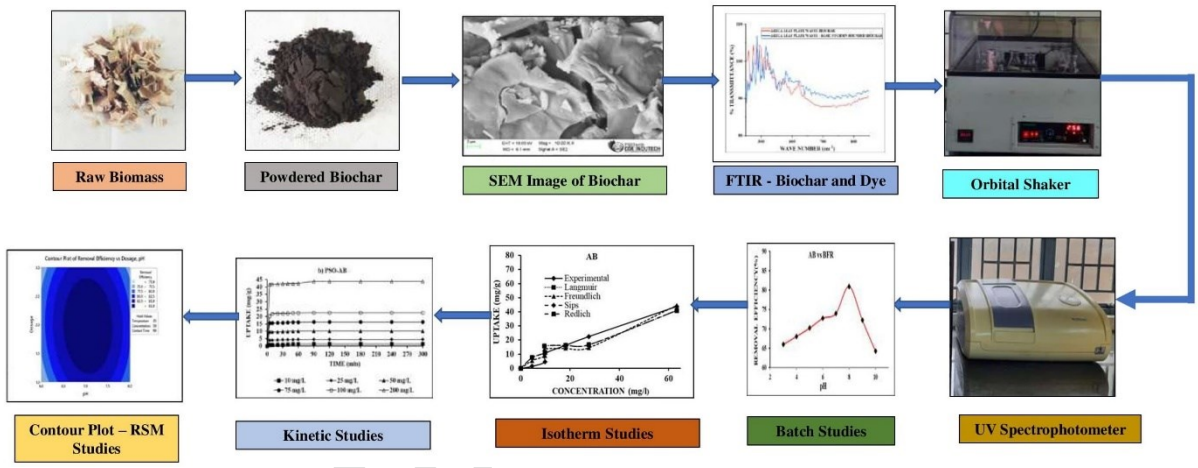

Abstract

In this study, the basic fusion dye was adsorbed from wastewater using turmeric leaf waste biochar and the experimental outcomes were fitted with isotherm and kinetics. Further, Response Surface Methodology (RSM) was also performed to analyse the concurrent interactive effects of the process variables. Pyrolysis of turmeric leaf waste biomass resulted in biochar yield of 44.65% at temperature of 300 °C. The biochar had moisture content of 4.21%, volatile matter of 45.38%, ash content of 17.74% and fixed carbon of 32.65% respectively. The batch adsorption studies showed maximum dye removal of 87.44 % and 71% at temperature of 35 °C, dosage of 0.3g, time of 60 min, pH of 7 and dye concentration of 50 ppm respectively for biochar and biomass respectively. The experimental data obtained at equilibrium condition fitted well in pseudo-second order and Langmuir isotherm with R^2 value

of 0.98 respectively. This study provides base for usage of turmeric leaf-based waste for synthesis of biochar and for effective removal of dye from aqueous environment.

Keywords: Turmeric leaf waste; Biochar; Red dye; Wastewater; Adsorption; RSM

1. Introduction

Dyes are widespread in use, making the environment and organisms prone to exposure through a lot of pathways such as food, water, soil and so on. Extensive research studies on the fate and hazards of dyes [1] have revealed that dyes are capable of causing environmental and biological hazards like eutrophication, destruction of aquatic flora and fauna, soil quality deterioration, mutagenicity, carcinogenic properties, genotoxicity, ecotoxicity, deformity induction and many more. This brings about an urgent need for more extensive and intense focus towards devising efficient methodologies for removal (or) treatment (or) degradation of dye-based contaminants in industrial effluents. Metal dye contaminants have been reported to have the ability to easily assimilate in and damage the respiratory organs of aquatic organisms. In particular, chromium dyes have been noted to be extremely tough to be traced and cause impediments in energy synthesis by plants [2].

Basic Red 9, also known as Basic Fuchsin Red is known to cause damage to DNA structures like tannery dyes do. It is also noteworthy that the aforementioned ability can also enable such dyes to be carcinogenic and cause cancer. Case in point, basic cationic dyes have been observed to cause bladder cancer. The usage of such dyes, particularly Basic Red 9 is widespread in textile industries which can be attributed to its efficiency in binding and as a colorant. The said properties of the dye makes the detection, tracing and removal of the same extremely difficult [3].

Development of research and technology over the years has increased awareness on the dangers of industrial effluents while making the scope for developing methods of treatment of the same simultaneously. Massive industrialisation entails developing and adapting to apt preventive measures. Various methods of dye effluent degradation are primarily classified into types based on the material and the mechanism involved, namely physical, chemical and biological. Adsorption, Ion exchange and Irradiation are some of the common physical dye degradation methods to name a few. Adsorption mechanism can be employed for removal of dyes wherein the contaminants travel from the effluent liquid phase to the adsorbent solid or liquid phase [4]. It is one of the most common methods for dye removal and even for general wastewater treatment [5]. Adsorption while generally classified under physical method of wastewater

treatment, is not strictly physical and falls under the physicochemical sector, which can be attributed to the complexity of the mechanism involved [6]. Conventional methods of adsorption include usage of carbon, modified carbon (activated carbon) and carbon-based derivatives like graphene, nano tubes as adsorbents [7].

The efficiency of adsorption process is often determined by the nature and quality of the adsorbent chosen. Therefore, selection of adsorbent is a crucial step in all adsorption processes, to ensure effective removal of the target pollutants or contaminants [8]. Apart from the type of adsorbent used, the universal factors that influence these processes are amount of contaminants present, temperature of the environment, pH of the effluent and the amount of adsorbent used [9]. Some of the most common conventional adsorbents used in the removal of dyes are commercial activated carbons, ion-exchange resins and inorganic adsorbents such as silica, activated alumina and synthetic zeolites/molecular sieves [10]. Turmeric leaf waste was renewable resource in Indian scenario. It was economical and bioresource when compared to traditionally used adsorbent source. It also possesses ease of operation during biochar production process. Also, it was clear from literature that biochar was effective on dye removal. Hence this resource was selected as adsorbent for removal of dye from aqueous solution. In literature, many common agricultural wastes such as date pits, wheat straw, peanut hull, rice and wheat husks, fruit and vegetable peels, corn cob, wood chips, sawdust and so on have been used in many studies as adsorbents for removing dyes and other pollutants like heavy metal ions and other organic compounds from wastewater [11][12].

In this study, the turmeric leaf waste biochar was synthesized via fast pyrolysis process under varying temperature range and the synthesized biochar was characterized using scanning electron microscope (SEM), Fourier transform infrared spectroscopy (FT-IR). The physio-chemical property of both biomass and biochar were analysed as per ASTM standards. Batch adsorption studies were performed to predict the optimum temperature, pH, time, adsorbent dosage and dye concentration. The experimental data were fitted with isotherm and kinetics studies to predict the adsorption capacity and mode of action. Further, the study was compared with response surface methodology.

2. Materials and methods

2.1 Raw material, adsorbent synthesis, and characterization

In this study, the biomass Turmeric leaf waste was collected from Sirumugai village, Coimbatore, Tamil Nadu was used for synthesis of biochar via fast pyrolysis. Biochar can be

prepared via hydrothermal carbonization and pyrolysis methods predominantly. When compared to other methods pyrolysis methods results in highly carbonaceous biochar. Also, the ash and volatile matter content are less in the biochar that are produced via pyrolysis methods. These are the backbone to select traditional methods for biochar preparation. The biomass was size reduced to even size of 1 mm using shredder before converting into biochar. Biomass was initially heated in hot air oven at 110 °C to ensure moisture content was below 5 wt%. About 10 g of moisture reduced biomass was heated in a stainless-steel reactor of 1 L capacity from 250 – 400 °C with heating rate of 10 °C/min for 1 h. The reactor was ensured to be in nitrogen environment during the process. After the temperature was reached the reactor was switched off and allowed to cool. Later, the samples were collected from the reactor and subjected to characterisation studies. In between each experiments, the reactor was sterilized to avoid contamination or loss of products [13]. The raw biomass and synthesized biochar were characterized through Scanning Electron Microscope (SEM), Zeta Potential, Fourier transform Infrared Spectroscopy (FT-IR) and X-ray Diffraction (XRD) as per ASTM standards. The proximate and elemental composition of both biomass and biochar was also estimated as per ASTM standards [14].

2.2 Wastewater

In this study, Basic fuchsin red dye (≥ 90.0% anhydrous basis, Sigma-Aldrich) was used to prepare dye wastewater. Wastewater stock solution (500 ppm) was prepared by mixing 0.5g of dye in 1 L of double distilled water. This solution serves as stock solution for performing various batch experiments. The dye concentration before and after the experiments were measured using UV-visible spectrophotometer (UV-1800 Shimadzu, Japan) at 546 nm [15].

2.3 Batch adsorption studies

Batch experiments were performed in 250 mL Erlenmeyer flasks and orbital shaker. Various parameters such as temperature (35, 40, 45 and 50 °C), pH (3 to 10), biochar dosage (1 to 10 g/L), dye concentration (10, 25, 50, 75, 100 and 200 ppm) and time (0 to 90 min) were studied during the study. During the experiments the flask was placed in orbital shaker and stirred at 200 rpm to attain equilibrium in mixing. The dye removal percentage was estimated as per Eq. (1).

$$Removal\ (\%) = \frac{C_o - C_e}{C_o} \times 100 \quad (1)$$

Where, C_o (mg/L) denotes the initial dye concentration and C_e (mg/L) is the equilibrium dye concentration at time t.

2.4 Isotherm and kinetics studies

Isotherm and kinetics studies were performed for the adsorption data obtained from above batch experiments. The isotherms that were fitted for the experimental data were Langmuir (Eq. (2)), Freundlich (Eq. (3)), Redlich-Peterson (Eq. (4)) and Sips (Eq. (5)) to depict the interaction of dye with biochar [16]. Adsorption kinetics like Pseudo-First order (Eq. (6)) and Pseudo Second order (Eq. (7)) were fitted for the adsorption data. This kinetics study helps to identify the adsorption capacity of biochar with respect to concentration of the solution.

$$\frac{C_e}{q_e} = \frac{C_e}{q_m} + \frac{1}{q_m b} \quad (2)$$

$$\log q_e = \log k_f + \left(\frac{1}{n}\right) \log C_e \quad (3)$$

$$q_e = K_{RP} C_e / (1 + \alpha_{RF} C_e \beta^{RP}) \quad (4)$$

$$q_e = K_s C_e^{\beta e} / (1 + \alpha_s C_e^{1/\beta s}) \quad (5)$$

$$q_t = q_e(1 - e^{-k_1 t}) \quad (6)$$

$$q_t = \frac{k_2 q_e^2}{1 + k_2 q_e t} \quad (7)$$

Where, q_e denotes adsorption capacity (mg/g), C_e is the concentration of dye at equilibrium (mg/L), b is the Langmuir constant (mg/g), k_f denotes the Freundlich constant, 1/n denotes the heterogeneity factor, q_t is amount of adsorption at time t, k_2 is second order constant, t is time, K_{RP} is Redlich-Peterson isotherm constant (L/g) and K_s is Sips model isotherm constant (L/g).

2.5 RSM

A reliable statistical tool employed to evaluate the concurrent interactive effects of various process variables on an output response is the response surface experimental design (RSM). This technique is proven to reduce the time and cost required for the experiments. In the present study, the Box-Behnken design of RSM was employed for optimizing five independent variables (Absorbent Dosage, pH, Temperature, Initial Dye Concentration and Contact Time) obtained from the experimental data for the efficient adsorption of Basic Fuchsin Red Dye [17]. The levels of each independent variables (Table.1) in the experiment were coded as -1 (Lower),

+1 (Upper), and 0 (Central), respectively. The polynomial model employed in the study can be represented as per Eq.8.

$$Y = R_o + \sum_{i=1}^{k} R_i X_i + \sum_{i=1}^{k-1} R_{jj} X_i^2 + \sum_{i=1}^{k} \sum_{j=2\ (i<j)}^{k} R_{iy} X_i X_j + \mathcal{E} \quad (8)$$

Wherein, Y is the response of the variables, X_i is the independent variables, R_0, R_i, R_j, R_{ij} are the known parameters (i = 1 - k, j = 1 - k), X_i and X_j are the coded levels of the variables, and Ɛ is the random error. The generated experimental results were analyzed and studied employing the ANOVA analysis expert 11 Stat-Ease Software.

Table 1 Ranges of Variable Factors at different levels of Box-Behnken model

S. No	Input Variables	Units	Levels		
			-1	0	1
1.	pH		6	7	8
2.	Dosage of Biochar	g	1	2	3
3.	Temperature	°C	30	35	40
4.	Initial Basic Fuchsin Red Dye Concentration	mg/L	25	50	75
5.	Contact Time	min	60	90	120

3. Results and discussion

3.1 Raw material and adsorbent characterization

The proximate analysis of biomass and biochar were analysed to predict the suitability of biochar for the adsorption process. The biomass and biochar had moisture content of 9.37 and 4.21 wt%, volatile matter of 74.18 and 45.38 wt%, ash content of 8.71 and 17.74 wt%, fixed carbon content of 7.73 and 32.65 wt% respectively. The elemental composition of biomass and biochar showed carbon of 56.22 and 66.13 wt%, nitrogen of 1.84 and 3.81wt%, oxygen of 41.92 and 29.98 wt%, sulphur of 0.02 and 0.07 wt% respectively. This data was supported by a recent literature, were the biochar had carbon of 85.3 %, hydrogen of 4.9 %, oxygen of 8.5 % respectively [18]. In another study with maple leaf, they reported presence of volatile matter of 59.5 %, ash content of 20.09% and fixed carbon of 19.60 % individually [19]. The high

amount of carbon formation was due to the processing of biomass at higher temperatures during biochar synthesis procedure.

The functional groups present in the raw biomass, biochar and spent biochar were analysed using FT-IR spectrum. FT-IR spectra of biochar, biomass and spent biochar were shown in fig.1. The presence of bands near to 800 cm^{-1} would have been due to the presence of C-H bonds attributed by the bending of aromatic compounds [20]. The peaks less than 500 cm^{-1} would have been due to Si-O groups [21]. Bands between 600 to 800 cm^{-1} would have been due to the presence of Fe-O stretching vibration [22].

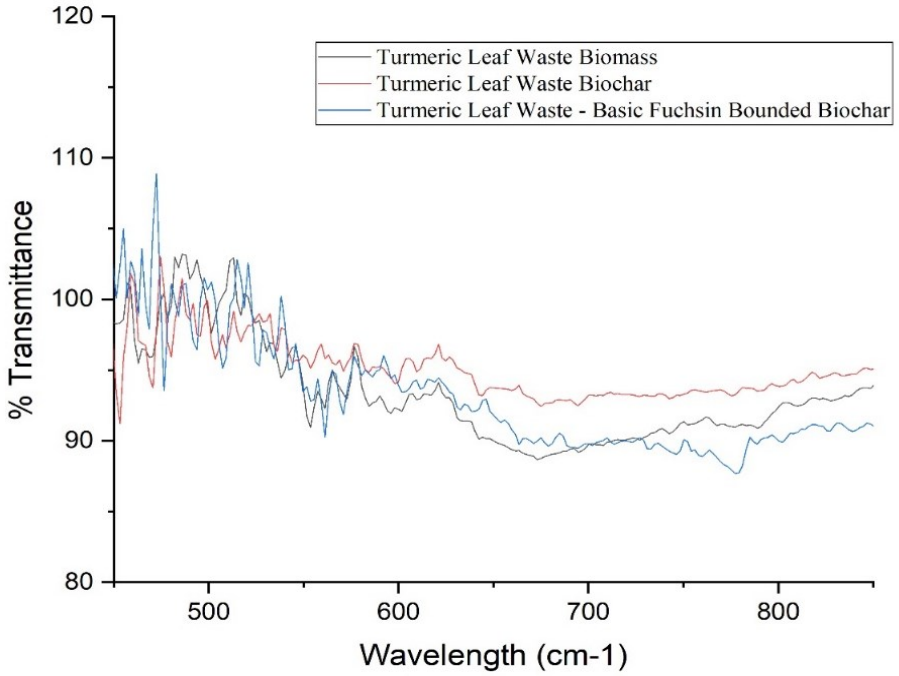

Fig.1 FT-IR spectrum of raw material, synthesized and spent biochar

The structural morphology of the biomass, biochar and spent biochar was analysed via Scanning Electron Microscope (SEM). The SEM image of biomass, biochar and spent biochar was shown in fig. 2, 3 and 4 respectively. It was clearly seen that after the pyrolysis process the surface of biomass got eroded and porous in structure. It was also clear that higher the pyrolysis temperature increased the change in surface morphology. Biochar was seen to have cuts and cracks after the pyrolysis process. The more the volatile matters released, higher the porosity and lesser density of the biochar. This helps to predict the dye removal process occurs through Vander Waals attraction, hydrogen bonding or electrostatic interaction [23]. Zeta potential values of biomass, and biochar were -12.7 mV and -10.1 mV respectively.

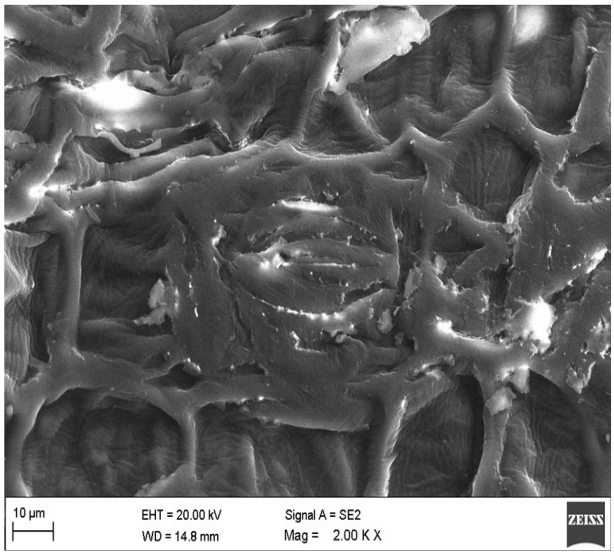

Fig. 2 SEM image of Turmeric Leaf waste

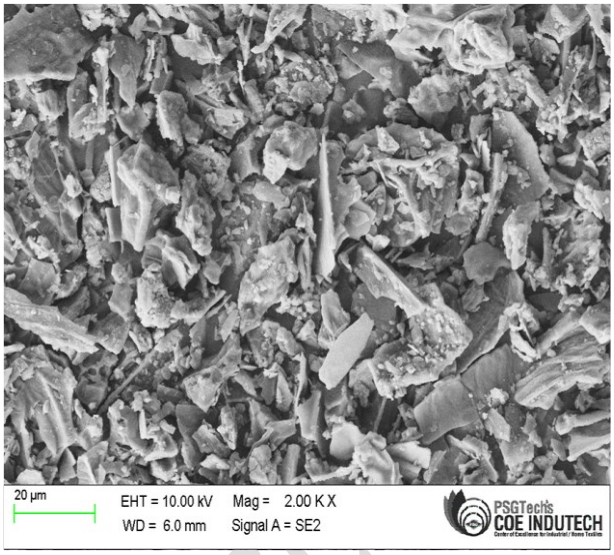

Fig. 3 SEM image of Turmeric Leaf biochar

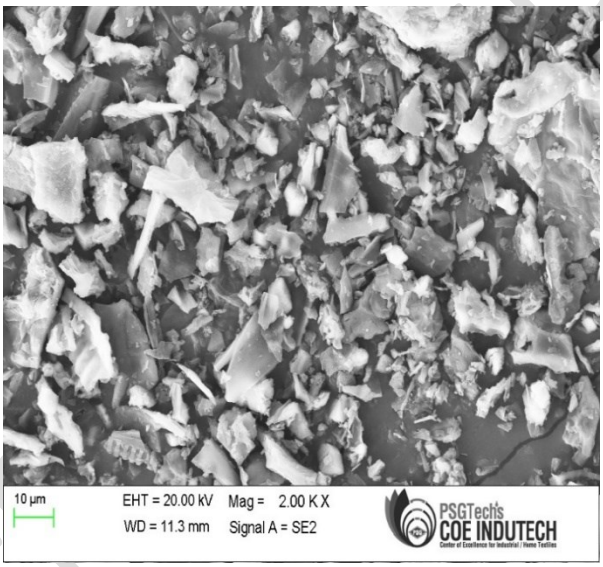

Fig. 4 SEM image of Basic Fuchsin dye Bounded Turmeric Leaf Waste Biochar

3.2 Effect of pyrolysis temperature on biochar yield

Pyrolysis temperature plays an important role in determining the yield of biochar. The biochar yield from the waste biomass was studied at varying temperature range like 250, 300, 350 and 400 °C respectively. The biochar yield was found to be 38.2, 44.6, 41.2 and 32.3 wt% at temperature of 250, 300, 350 and 400 °C respectively. The optimum temperature for maximum biochar yield was 300 °C, beyond that yield reduced. This may be due to degradation of ash and other volatile components present in the biochar. In another study, distilled stillage resulted in biochar yield of 50.7 % via slow pyrolysis at 45 min and 370 °C [24]. Similarly, rice husk

upon pyrolysis at 300 °C resulted in biochar yield of 37.71 % and time of 90 min respectively [25].

3.3 Batch experiments

3.3.1 Concentration of dye on adsorption

The effect of dye concentration on removal efficiency was estimated via batch experiments and the results were shown in fig.5. The batch dose experiments were carried out in varying dye concentrations like 10, 25, 50, 75, 100 and 200 mg/L under constant conditions like pH of 7, temperature of 35 °C, dosage of 0.3g, time of 60 min. From the results, it was seen that biochar resulted in higher (77.60 %) dye removal percentage than biomass (60.6 %). It was found that increase in initial dye concentration increases the competition in occupying the active sites present in the adsorbent. Accumulation of dye molecules in the active sites decreases the removal percentage.

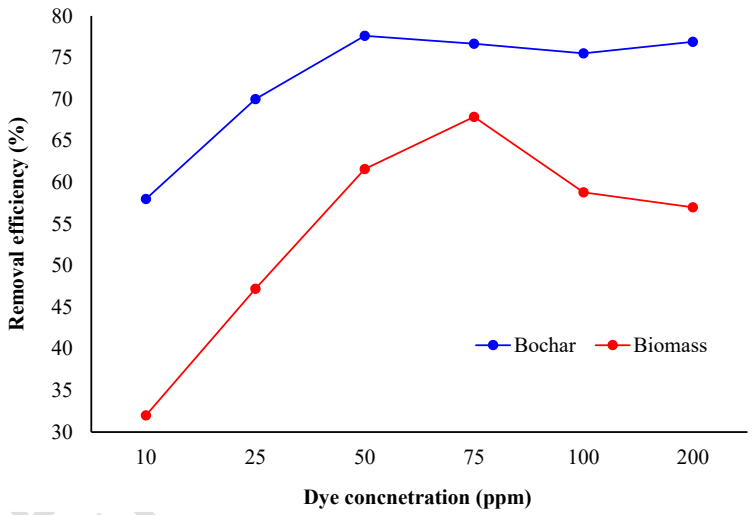

Fig. 5. Effect of varying dye concentration on dye removal efficiency

3.3.2 Dosage

The batch sorption studies were performed under pH of 7, temperature of 35 °C, dye concentration of 50 ppm and time of 60 min to determine the dye removal efficiency. The effect of adsorbent dosage on dye removal was studies at varying dosage concentration of 1 to 10 g/L and shown in fig.6. From the results, it was seen that the maximum dye removal of 80.4% for biochar and 68% at 0.4g and 0.6g dosage. However, the optimum concentration was found to be 0.3g, where the removal percentage was 79.6 and 58%. Beyond 0.3g there were no notable significant increase in dye removal was seen. Our study was supported with literature, in which the main reason for dye removal was found that the increase in adsorbent dosage increased the

presence of active sites, which resulted in enhanced dye removal [26]. In a study, crystal violet dye was removed to 86.4 % by biochar obtained from palm kernel shells [27].

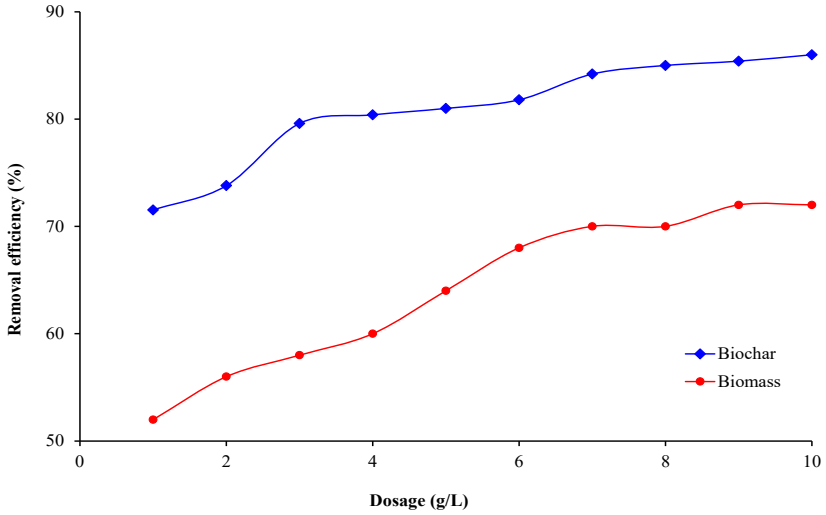

Fig.6 Effect of adsorbent dosage on removal efficiency

3.3.3 Time

The role of time on dye removal efficiency was studied with series of batch experiments under constant conditions like temperature of 35 °C, dosage of 0.3g, pH of 7 and dye concentration of 50 ppm respectively. The time dependant graph was shown in fig. 7. From the results, it was clear that the increase in exposure of dye to adsorbent at loner time period increased the dye removal percentage. The maximum dye removed was 87.55 and 55% at 60 min for biochar and biomass respectively. Beyond 60 min, there were no significant increase dye removal efficiency. This would have been due to unavailability of active sites and longer exposure of adsorbent and dye.

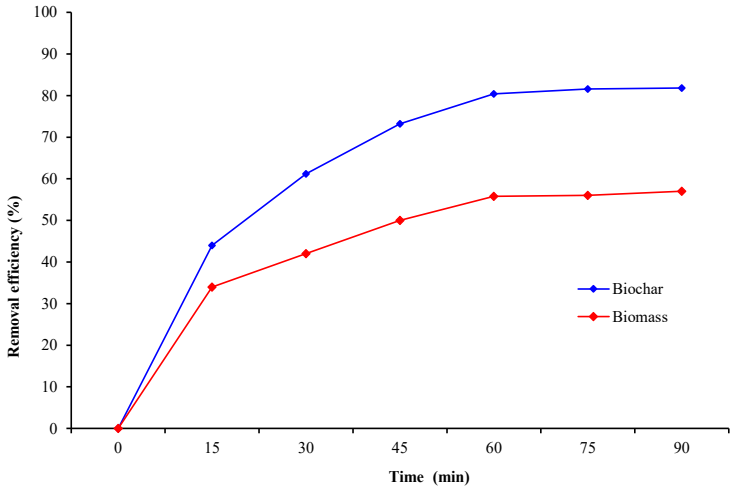

Fig.7. Time dependant removal of dye by biochar and biomass

3.3.4 pH

The batch experiments were performed to analyse the pH sensitivity of biochar and biomass in removal of dye under conditions like temperature of 35 °C, dosage of 0.3g, time of 60 min, and dye concentration of 50 ppm respectively. The results of dye removal efficiency at varying pH concentration (3 to 8) were shown in fig. 8. From the results, it was seen that the maximum dye removal occurred in between pH of 5 to 7. At acidic condition (pH of 3), the dye removal efficiency for biochar and biomass was 64 and 50% respectively. The dye removal efficiency increased to 79 and 62 % at pH of 7, whereas at alkaline conditions the dye removal efficiency slightly reduced to 76 and 58 % respectively. It was reported that increase in pH of the solution reduces the ionization potential of the functional groups of the adsorbent [16]. In that study, they reported that increase in pH to alkaline condition decreased the malachite green dye removal efficiency to 76 % from 96 % respectively.

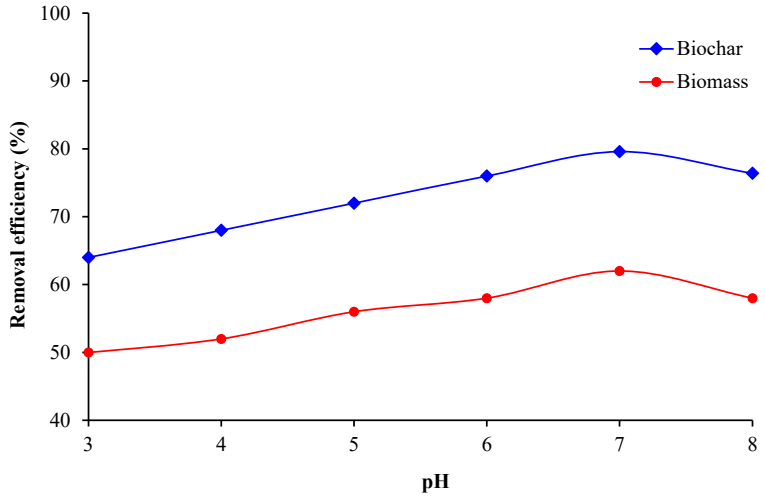

Fig.8. Effect of pH on dye removal efficiency

3.3.5 Temperature

The temperature plays an important role in any kind of experiments. The batch experiments on estimating the dye removal percentage were conducted under constant conditions like dosage of 0.3g, time of 60 min, pH of 7 and dye concentration of 50 ppm respectively. The effect of temperature on dye removal was shown in fig.9. The maximum dye removal percentage was 83 and 71% at 35 °C for biochar and biomass respectively. Increase in temperature to 50 °C resulted in decrease in dye removal efficiency to 63 and 51% for biochar and biomass

individually. This may be due to the breaking of bond between dye and adsorbent under higher temperature.

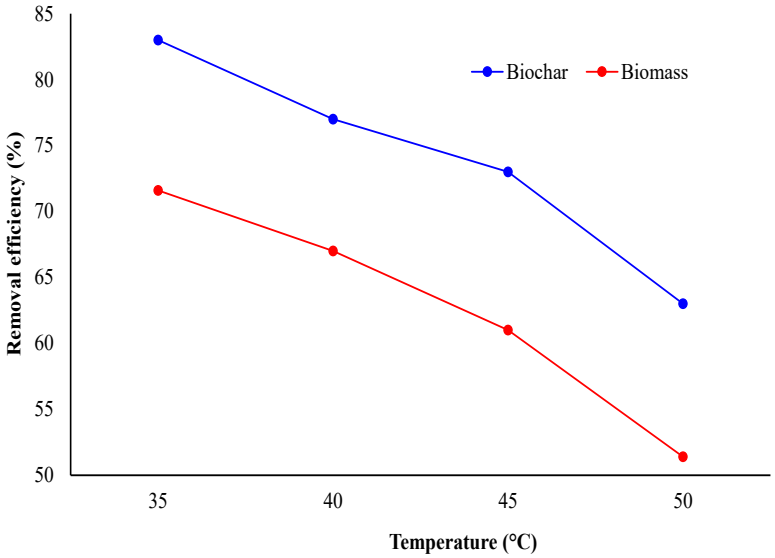

Fig.9. Effect of temperature on dye removal by biochar and biomass

This results in ineffectiveness of electrostatic forces at higher movement of molecules at higher temperature. In another study, it was reported that the *Murraya Koenigii* stem biochar removed 96.6 % of crystal violet dye at 35 °C [28].

3.4 Isotherm and kinetics

Adsorption isotherm models are performed for the data obtained at equilibrium conditions to predict the number of molecules distributed between the solid and liquid medium. In our study, we performed isotherm model analysis for biochar and basic fuchsin red dye, since biochar showed better removal efficiency than biomass. Fig. 10, depicts the linearized isotherm equation for varying initial dye concentration of 0 – 60 mg/L respectively. The isotherm constants obtained by fitting the equilibrium data was shown in Table. 2. From Table. 2, based on the values of R^2 the adsorption isotherm was: Langmuir > Sips > Redlich-Peterson > Freundlich for AB biochar respectively. It was clear that Freundlich, Sips, and Redlich-Peterson models were not giving the best fit for the obtained experimental data as their R^2 value (R^2 = 0.91, 0.96, 0.95) are less when compared to Langmuir isotherm model (R^2 = 0.98). This indicates that the adsorption of red dye by biochar has occurred via monolayer adsorption manner (monolayer adsorption capacity (q_m) was found out to be 283321.29 mg/g). The energy of adsorption is uniform throughout the adsorbed layer on the biochar adsorbent surface, at a constant temperature.

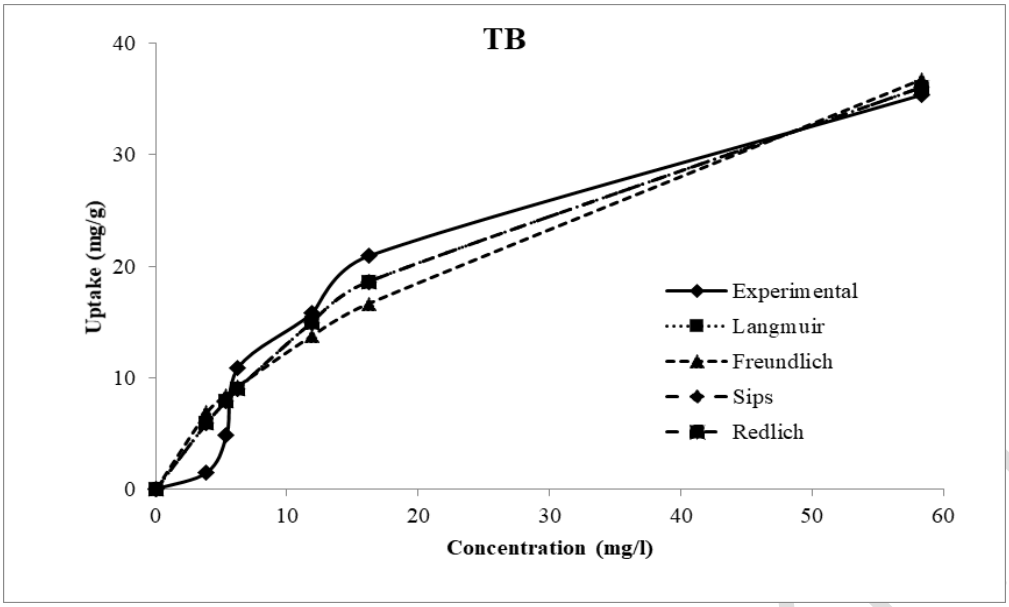

Fig. 10. Various isotherm graph of Turmeric Leaf Waste Biochar

Table 2. Isotherm Constants, Regression Co-efficient and percentage error for Turmeric Leaf Waste Biochar

Langmuir		**q_m, (mg/g)**	**Ka**	**R^2**	**% Error**
		283.3212	0.029	0.98	44.49
Freundlich		**K_F**	**1/n**	**R^2**	**% Error**
		2.97	0.61	0.91	31.12
Redlich	**Krp**	**aRP**	**βRP**	**R^2**	**% Error**
	1.71	0.030	1	0.95	32.16
Sips	**Ks**	**as**	**Bs**	**R^2**	**% Error**
	1.71	0.03	1	0.96	32.15

Adsorption kinetics was performed to predict the reaction pathway and dye removal rate from the dye wastewater. The pseudo-first and pseudo-second order kinetics plots for the AB biochar were shown in Fig. 11 and 12. The regression coefficient and rate constants (q_{eq}, K_1, R_2 and % error) of the experimental data are tabulated in Table. 3. In our study, we obtained an experimental uptake (q_e) value of 21.61 mg/g at 50 mg/L which is approximately similar to calculated q_e of both the pseudo-first and pseudo-second order kinetics for AB biochar. From the results, it was seen that pseudo-second order kinetics showed regression coefficient value of 0.99 as better than pseudo-first order kinetics for biochar. In another study, Palm Kernel Shell-Derived biochar was used to remove crystal violet dye from textile wastewater and it was

reported that it showed pseudo-second order kinetics and Langmuir isotherm model which is very much similar to our present study [29].

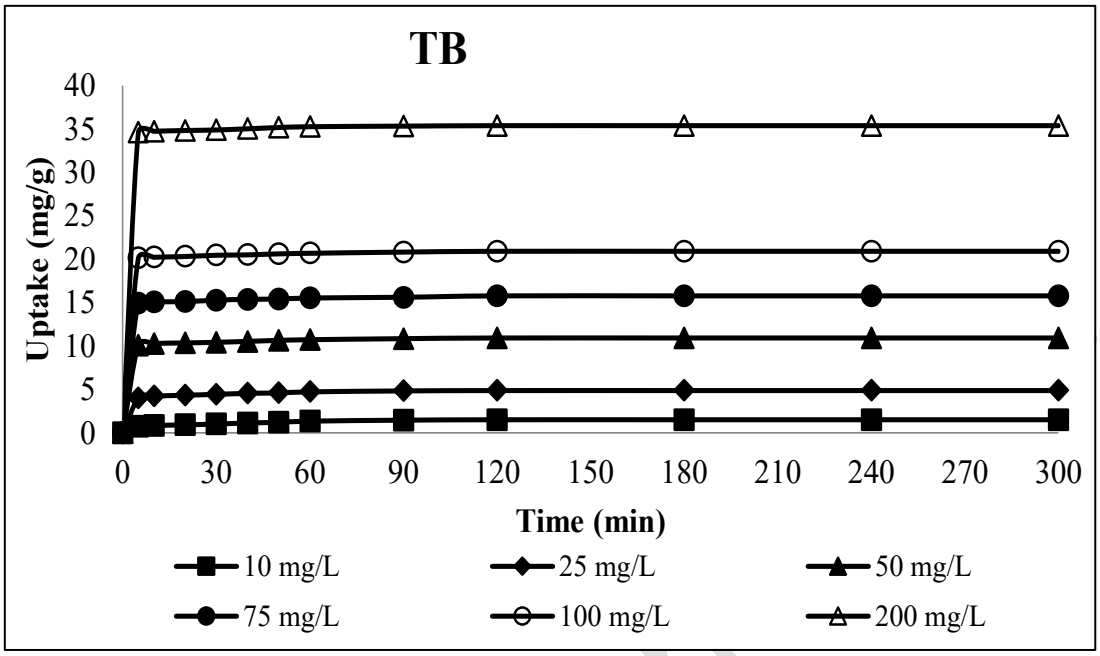

Fig. 11. Kinetics plot (pseudo first order) for TB biochar bounded on BFR Dye

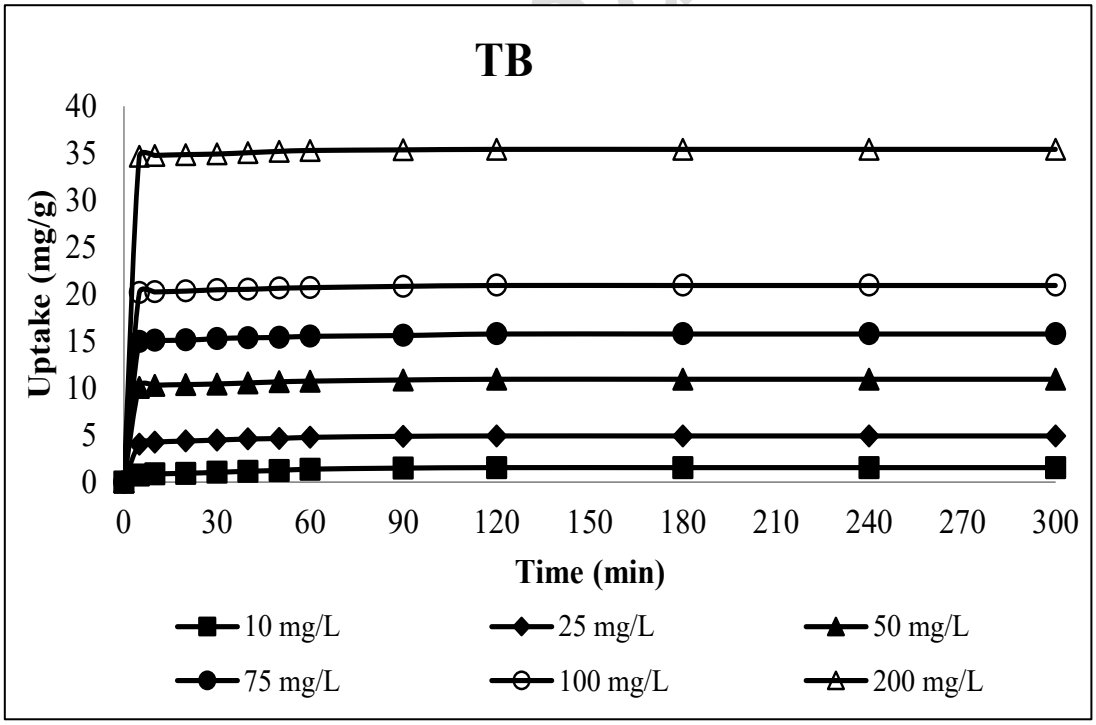

Fig. 12. Kinetics plot (pseudo second order) for TB biochar bounded on BFR Dye

Table 3 **Kinetic parameters of Pseudo First and Second order models of Turmeric Leaf Waste Biochar**

C_o (mg/L)	Pseudo First Order Model				Pseudo Second Order Model			
	q_{eq} (mg/g)	K_1 (1/min)	R^2	% Error	q_{eq} (mg/g)	K_2 (1/min)	R^2	% error
10	2.82	4.86	0.90	7.88	3.25	0.08	0.98	2.65
25	9.59	4.86	0.99	2.15	10.00	0.11	0.99	0.90
50	21.61	4.86	0.99	1.05	22.02	0.11	0.99	0.43
75	31.31	4.86	0.99	0.66	31.71	0.11	0.99	0.24
100	41.63	4.86	0.99	0.52	41.99	0.12	0.99	0.17
200	70.59	4.86	0.99	0.28	70.99	0.12	0.99	0.11

3.5 RSM

RSM was the collection of the statistical and mathematical methods on demonstrating, investigating and modelling the issues raised. This technique is used to analyze and study the relationship between variables (Dependent and Independent) and to study the enhancement of the rate of the reaction when variables are shifted at same time [30]. The variation in the combination of variables results in a greater amount of product formation, and the corresponding responses were optimized [31]. Currently, the application of RSM in the field of adsorption experiments is flourishing. The study was conducted to analyze and study the effect of Dosage of Turmeric Leaf Waste Biochar, pH, Temperature, and Initial Basic Fuchsin Red Dye Concentration, and Contact Time on the removal efficiency using five independent variables at three different levels. Around 46 experiments were conducted in a random order to determine the co-efficient of the model. The obtained results are elaborated in removal efficiency % in Table 4.

From the results, it can be seen that the highest upgraded removal efficiency was obtained as 87.44 % at pH of 7, Adsorbent Dosage of 2 g, Temperature of 35 °C, Concentration of 50 mg/L, and Contact time of 90 min. Whereas the lowest removal efficiency was obtained as 75.45 %. The Analysis of Variance (ANOVA) of the current study is depicted in the Table. 5. The interaction element's P value is quite high, and it indicated that it is of less significance. To predict the response of each factor at given levels, equations with coded and actual values were used. The final equation in terms of removal efficiency is represented as per Eq.9.

Removal Efficiency

$$= -463.2 + 114.1\,A + 25.47\,B + 4.13\,C + 0.627\,D + 0.743\,E - 8.002\,A*A - 3.570\,B*B - 0.0407\,C*C - 0.002886\,D*D - 0.001066\,E*E - 0.475A*B - 0.010\,A*C + 0.0000\,A*D - 0.0000\,A*E - 0.087\,B*C + 0.0010\,B*D - 0.0558\,B*E - 0.00500\,C*D - 0.00875\,C*E - 0.00193\,D*E \quad (9)$$

From equation 9, The terms A (pH), B (Dosage), C (Temperature), D (Concentration) and E (Contact time) are linear, the terms AB, AC, AD, BC, BD, CD, AE, BE, CE and DE are interactions, terms and AA, BB, CC, DD and EE are Square. The polynomial second order regression has a combination of above said terms. All linear terms and interaction BD only provide positive results over other terms that are negative. The factor A, B, C, D and BD are most influencing process variables over other factors and coefficient of pH has a significant effect on the upgraded removal efficiency. Hence, the beta coefficients are positive and negative signs. One more reason for positive interaction is that the sum of mean squares is high on positive sign factors. The surface plots of the Removal Efficiency for the removal of Basic Fuchsin Red Dye by the Turmeric Leaf Waste Biochar on varying the five-independent variable in a 2-way interaction is shown in Fig.13 to 22.

Table 4 Design Matrix for Upgraded Removal Efficiency

Std Order	Run Order	Pt Type	Block	pH	Dosage	Temperature	Concentration	Contact Time	Target	Error (%)
41	1	0	1	7	2	35	50	90	87.44	0
40	2	2	1	7	3	35	75	90	82.35	5.82
27	3	2	1	6	2	35	75	90	76.97	11.97
19	4	2	1	7	2	35	25	120	87.44	0.00
24	5	2	1	7	3	40	50	90	83.28	4.76
14	6	2	1	8	2	30	50	90	78.88	9.79
10	7	2	1	7	3	35	50	60	82.35	5.82
9	8	2	1	7	1	35	50	60	80.74	7.66
44	9	0	1	7	2	35	50	90	87.44	0
32	10	2	1	7	2	40	50	120	87.44	0
30	11	2	1	7	2	40	50	60	87.44	0
38	12	2	1	7	3	35	25	90	82.35	5.82
35	13	2	1	6	2	35	50	120	76.97	11.97
7	14	2	1	7	2	30	75	90	87.44	0.00
25	15	2	1	6	2	35	25	90	76.97	11.97
16	16	2	1	8	2	40	50	90	78.68	10.02
5	17	2	1	7	2	30	25	90	87.44	0

26	18	2	1	8	2	35	25	90	78.68	10.02
4	19	2	1	8	3	35	50	90	75.83	13.28
13	20	2	1	6	2	30	50	90	76.97	11.97
11	21	2	1	7	1	35	50	120	87.44	0
28	22	2	1	8	2	35	75	90	78.68	10.02
1	23	2	1	6	1	35	50	90	76.97	11.97
31	24	2	1	7	2	30	50	120	87.44	0
23	25	2	1	7	1	40	50	90	82.65	5.48
46	26	0	1	7	2	35	50	90	87.44	0
43	27	0	1	7	2	35	50	90	87.44	0
6	28	2	1	7	2	40	25	90	84.37	3.51
37	29	2	1	7	1	35	25	90	80.77	7.63
3	30	2	1	6	3	35	50	90	75.45	13.71
29	31	2	1	7	2	30	50	60	82.19	6.00
8	32	2	1	7	2	40	75	90	81.87	6.37
18	33	2	1	7	2	35	75	60	84.16	3.75
2	34	2	1	8	1	35	50	90	79.25	9.37
17	35	2	1	7	2	35	25	60	81.66	6.61
39	36	2	1	7	1	35	75	90	80.67	7.74
21	37	2	1	7	1	30	50	90	79.99	8.52
22	38	2	1	7	3	30	50	90	82.35	5.82

36	39	2	1	8	2	35	50	120	78.68	10.02
20	40	2	1	7	2	35	75	120	84.16	3.75
34	41	2	1	8	2	35	50	60	78.68	10.02
33	42	2	1	6	2	35	50	60	76.97	11.97
12	43	2	1	7	3	35	50	120	82.35	5.82
42	44	0	1	7	2	35	50	90	87.44	0
45	45	0	1	7	2	35	50	90	87.44	0
15	46	2	1	6	2	40	50	90	76.97	11.97

Table 5 ANOVA Table

Source	DF	Adj. SS	Adj. MS	F-Value	P-Value
Model	20	675.973	33.799	12.91	0.000
Linear	5	31.414	6.283	2.40	0.066
pH	1	10.758	10.758	4.11	0.053
Dosage	1	0.294	0.294	0.11	0.740
Temperature	1	0.000	0.000	0.00	1.000
Concentration	1	0.714	0.714	0.27	0.606
Contact Time	1	19.647	19.647	7.50	0.011
Square	5	614.868	122.974	46.96	0.000
pH*pH	1	558.836	558.836	213.38	0.000
Dosage*Dosage	1	111.202	111.202	42.46	0.000
Temperature*Temperature	1	9.058	9.058	3.46	0.075
Concentration*Concentration	1	28.394	28.394	10.84	0.003
Contact Time*Contact Time	1	8.036	8.036	3.07	0.092
2-Way Interaction	10	29.691	2.969	1.13	0.378
pH*Dosage	1	0.902	0.902	0.34	0.562
pH*Temperature	1	0.010	0.010	0.00	0.951
pH*Concentration	1	0.000	0.000	0.00	1.000
pH*Contact Time	1	0.000	0.000	0.00	1.000
Dosage*Temperature	1	0.748	0.748	0.29	0.598
Dosage*Concentration	1	0.002	0.002	0.00	0.976
Dosage*Contact Time	1	11.223	11.223	4.29	0.049
Temperature*Concentration	1	1.562	1.562	0.60	0.447
Temperature*Contact Time	1	6.891	6.891	2.63	0.117
Concentration*Contact Time	1	8.352	8.352	3.19	0.086
Error	25	65.474	2.619		
Lack-of-Fit	20	65.474	3.274	*	*
Pure Error	5	0.000	0.000		
Total	45	741.447			

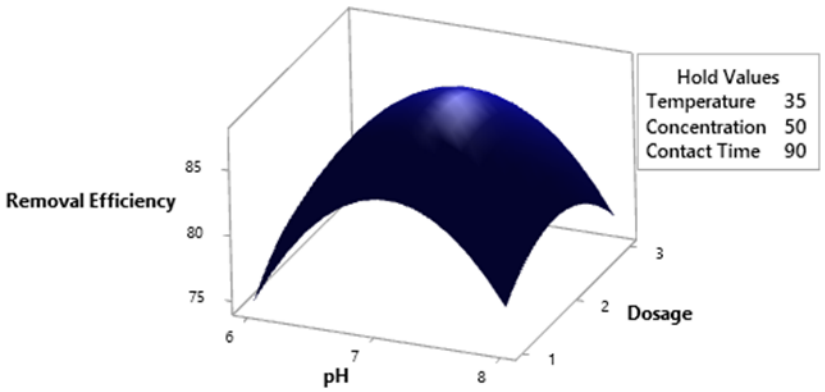

Fig. 13. Surface Plot of Removal Efficiency vs Dosage & pH

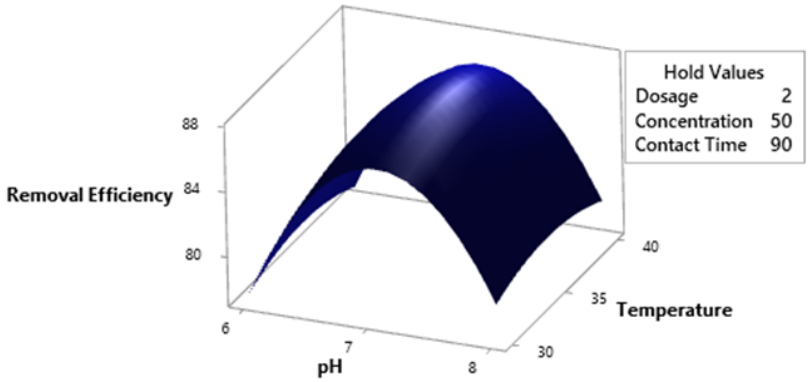

Fig. 14. Surface Plot of Removal Efficiency vs Temperature & pH

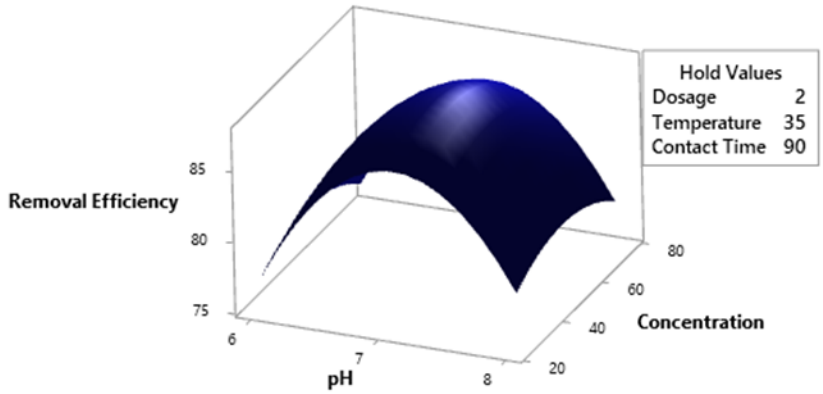

Fig. 15. Surface Plot of Removal Efficiency vs Concentration & pH

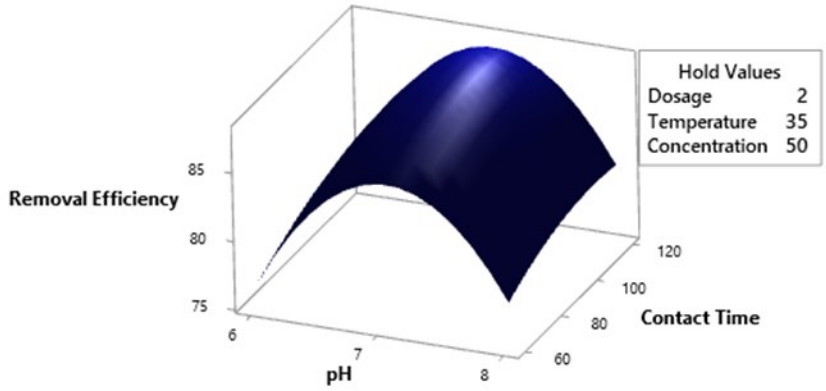

Fig. 16. Surface Plot of Removal Efficiency vs Contact Time & pH

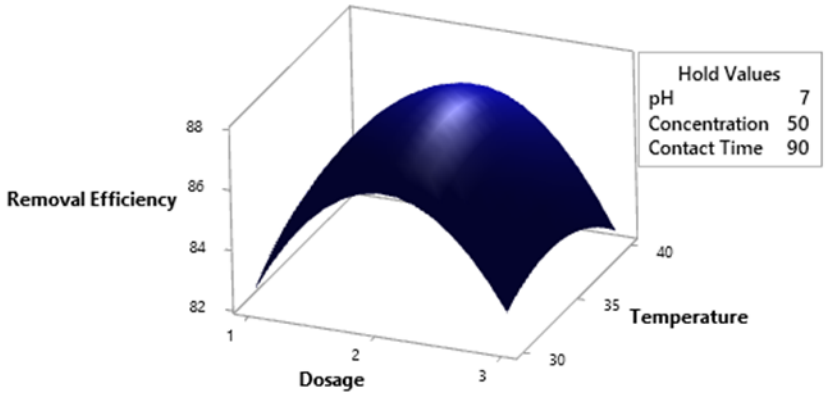

Fig. 17. Surface Plot of Removal Efficiency vs Temperature & Dosage

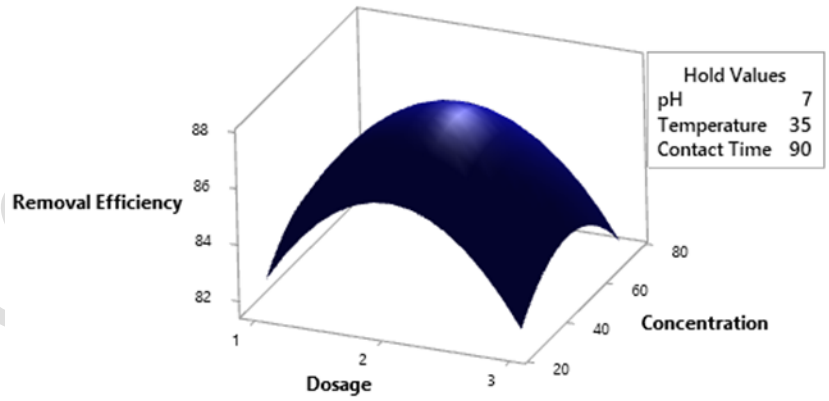

Fig. 18. Surface Plot of Removal Efficiency vs Concentration & Dosage

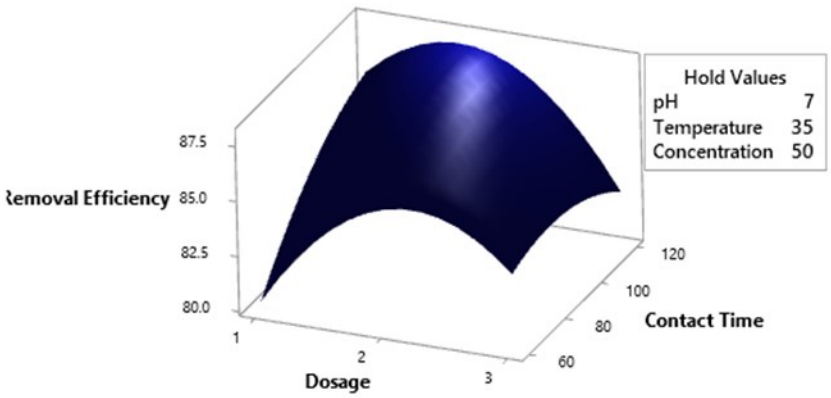

Fig. 19. Surface Plot of Removal Efficiency vs Contact Time & Dosage

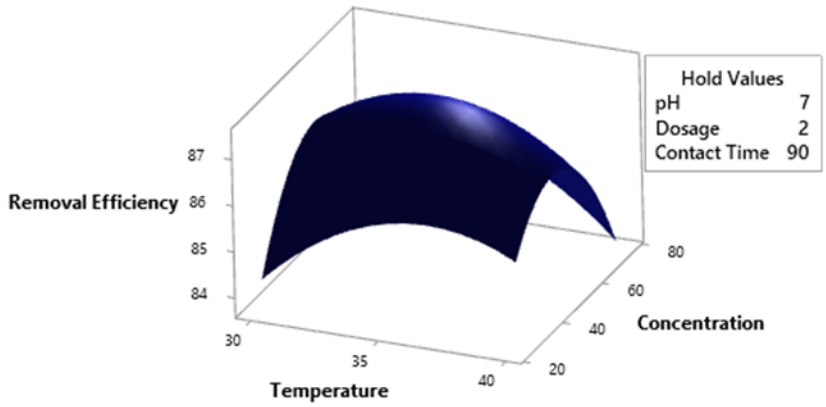

Fig. 20. Surface Plot of Removal Efficiency vs Concentration & Temperature

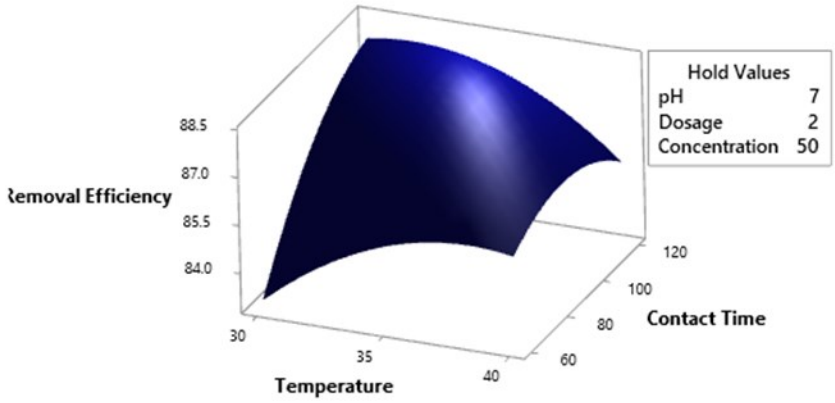

Fig. 21. Surface Plot of Removal Efficiency vs Contact Time & Temperature

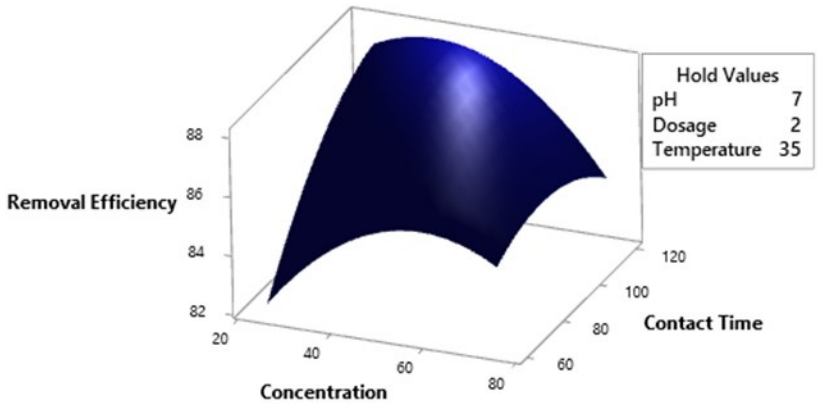

Fig. 22. Surface Plot of Removal Efficiency vs Contact Time & Concentration

4. Conclusion

In this study, pyrolysis process was used to convert turmeric leaf biomass into biochar. The biochar yield was 44.65% at temperature of 300 °C and it comprised volatile matter, moisture, ash and fixed carbon of 45.38, 4.21, 17.74 and 32.65% respectively. Biochar had well developed cracks and pores on the surface as result of the pyrolysis temperature conditions. The adsorption studies of turmeric leaf biochar on red dye showed maximum dye removal of 83 % at temperature of 35 °C, dosage of 0.3g, time of 60 min, pH of 7 and dye concentration of 50 ppm respectively. The experimental data obtained at equilibrium conditions were fitted via isotherm and kinetics studies and it best fitted with Langmuir isotherm with R^2 of 0.98 and Pseudo second order. Further using RSM, the concurrent interactive effects of various process variables on an output response were analysed. This study provided promising results in controlled conditions; in future it has to be expanded to real time applications.

Conflicts of interest

The authors declare no conflict of interest.

References

[1] S. Madhav, A. Ahamad, P. Singh, P.K. Mishra, A review of textile industry: Wet processing, environmental impacts, and effluent treatment methods, Environ. Qual. Manag. 27 (2018) 31–41. https://doi.org/10.1002/tqem.21538.

[2] B. Lellis, C.Z. Fávaro-Polonio, J.A. Pamphile, J.C. Polonio, Effects of textile dyes on health and the environment and bioremediation potential of living organisms, Biotechnol. Res. Innov. 3 (2019) 275–290. https://doi.org/10.1016/j.biori.2019.09.001.

[3] B.K. Nandi, S. Patel, Removal of Pararosaniline Hydrochloride Dye (Basic Red 9) from Aqueous Solution by Electrocoagulation:Experimental, Kinetics, and Modeling, J. Dispers. Sci. Technol. 34 (2013) 1713–1724. https://doi.org/10.1080/01932691.2013.767203.

[4] C.B. Crawford, B. Quinn, The interactions of microplastics and chemical pollutants, in: Microplastic Pollut., Elsevier, 2017: pp. 131–157. https://doi.org/10.1016/b978-0-12-809406-8.00006-2.

[5] V.K. Gupta, Suhas, Application of low-cost adsorbents for dye removal - A review, J. Environ. Manage. 90 (2009) 2313–2342. https://doi.org/10.1016/j.jenvman.2008.11.017.

[6] K.Y. Foo, B.H. Hameed, An overview of dye removal via activated carbon adsorption process, Desalin. Water Treat. 19 (2010) 255–274. https://doi.org/10.5004/dwt.2010.1214.

[7] G.Z. Kyzas, K.A. Matis, Nanoadsorbents for pollutants removal: A review, J. Mol. Liq. 203 (2015) 159–168. https://doi.org/10.1016/j.molliq.2015.01.004.

[8] U. Ozdemir, I. Ozbay, B. Ozbay, S. Veli, Application of economical models for dye removal from aqueous solutions: Cash flow, cost-benefit, and alternative selection methods, Clean Technol. Environ. Policy. 16 (2014) 423–429. https://doi.org/10.1007/s10098-013-0638-y.

[9] M.T. Yagub, T.K. Sen, S. Afroze, H.M. Ang, Dye and its removal from aqueous solution by adsorption: a review. Adv Colloid Interfac 209: 172--184, (2014).

[10] G. Crini, E. Lichtfouse, L.D. Wilson, N. Morin-Crini, Conventional and non-conventional adsorbents for wastewater treatment, Environ. Chem. Lett. 17 (2019) 195–

213. https://doi.org/10.1007/s10311-018-0786-8.

[11] K.A. Adegoke, O.S. Bello, Dye sequestration using agricultural wastes as adsorbents, Water Resour. Ind. 12 (2015) 8–24. https://doi.org/10.1016/j.wri.2015.09.002.

[12] L. Bulgariu, L.B. Escudero, O.S. Bello, M. Iqbal, J. Nisar, K.A. Adegoke, F. Alakhras, M. Kornaros, I. Anastopoulos, The utilization of leaf-based adsorbents for dyes removal: A review, J. Mol. Liq. 276 (2019) 728–747. https://doi.org/10.1016/j.molliq.2018.12.001.

[13] S.Y. Foong, R.K. Liew, Y. Yang, Y.W. Cheng, P.N.Y. Yek, W.A.W. Mahari, X.Y. Lee, C.S. Han, D.-V.N. Vo, Q. Van Le, Valorization of biomass waste to engineered activated biochar by microwave pyrolysis: progress, challenges, and future directions, Chem. Eng. J. 389 (2020) 124401.

[14] J. Arun, K.P. Gopinath, R. Sivaramakrishnan, P. SundarRajan, R. Malolan, A. Pugazhendhi, Technical insights into the production of green fuel from CO2 sequestered algal biomass: A conceptual review on green energy, Sci. Total Environ. (2020) 142636.

[15] M.A. Ahmad, N.S. Afandi, K.A. Adegoke, O.S. Bello, Optimization and batch studies on adsorption of malachite green dye using rambutan seed activated carbon, Desalin. Water Treat. 57 (2016) 21487–21511. https://doi.org/10.1080/19443994.2015.1119744.

[16] P. Ganguly, R. Sarkhel, P. Das, Synthesis of pyrolyzed biochar and its application for dye removal: Batch, kinetic and isotherm with linear and non-linear mathematical analysis, Surfaces and Interfaces. 20 (2020) 100616. https://doi.org/10.1016/j.surfin.2020.100616.

[17] G. Vyavahare, P. Jadhav, J. Jadhav, R. Patil, C. Aware, D. Patil, A. Gophane, Y.H. Yang, R. Gurav, Strategies for crystal violet dye sorption on biochar derived from mango leaves and evaluation of residual dye toxicity, J. Clean. Prod. 207 (2019) 296–305. https://doi.org/10.1016/j.jclepro.2018.09.193.

[18] J. Arun, K.P. Gopinath, S.S. Vigneshwar, A. Swetha, Sustainable and eco-friendly approach for phosphorus recovery from wastewater by hydrothermally carbonized microalgae: study on spent bio-char as fertilizer, J. Water Process Eng. 38 (2020) 101567.

[19] J.E. Kim, S.K. Bhatia, H.J. Song, E. Yoo, H.J. Jeon, J.-Y. Yoon, Y. Yang, R. Gurav, Y.-

H. Yang, H.J. Kim, Adsorptive removal of tetracycline from aqueous solution by maple leaf-derived biochar, Bioresour. Technol. 306 (2020) 123092.

[20] A. Allwar, others, Removal of 2-Chlorophenol using Rice Husk Activated Carbon Prepared by ZnCl2/H3PO4 Activation, Orient. J. Chem. 33 (2017) 2386.

[21] M.A.A. Rahim, M.M. Ismail, A.M.A. Mageed, Production of activated carbon and precipitated white nanosilica from rice husk ash,'', Int. J. Adv. Res. 3 (2015) 491–498.

[22] A.O. Dada, F.A. Adekola, E.O. Odebunmi, Synthesis and characterization of iron nanoparticles and its ash rice husk supported nanocomposite, in: Proc. 1st African Int. Conf. Appl. Nanotechnol. to Energy, Heal. Environ. UNN, 2014.

[23] A. Ray, A. Banerjee, A. Dubey, Characterization of biochars from various agricultural by-products using FTIR spectroscopy, SEM focused with image processing, Int. J. Agric. Environ. Biotechnol. 13 (2020) 423–430.

[24] S. Ghysels, F. Ronsse, D. Dickinson, W. Prins, Production and characterization of slow pyrolysis biochar from lignin-rich digested stillage from lignocellulosic ethanol production, Biomass and Bioenergy. 122 (2019) 349–360. https://doi.org/https://doi.org/10.1016/j.biombioe.2019.01.040.

[25] F.R. Vieira, C.M. Romero Luna, G.L.A.F. Arce, I. Ávila, Optimization of slow pyrolysis process parameters using a fixed bed reactor for biochar yield from rice husk, Biomass and Bioenergy. 132 (2020) 105412. https://doi.org/https://doi.org/10.1016/j.biombioe.2019.105412.

[26] N.M. Mahmoodi, M. Taghizadeh, A. Taghizadeh, Ultrasound-assisted green synthesis and application of recyclable nanoporous chromium-based metal-organic framework, Korean J. Chem. Eng. 36 (2019) 287–298.

[27] P.P. Kyi, J.O. Quansah, C.-G. Lee, J.-K. Moon, S.-J. Park, The Removal of Crystal Violet from Textile Wastewater Using Palm Kernel Shell-Derived Biochar, Appl. Sci. . 10 (2020). https://doi.org/10.3390/app10072251.

[28] A. Saniya, K. Sathya, K. Nagarajan, M. Yogesh, H. Jayalakshmi, P. Praveena, S. Bharathi, Modelling of the removal of crystal violet dye from textile effluent using murraya koenigii stem biochar, Desalin. Water Treat. 203 (2020) 356–365. https://doi.org/10.5004/dwt.2020.26191.

[29] P.P. Kyi, J.O. Quansah, C.G. Lee, J.K. Moon, S.J. Park, The removal of crystal violet from textile wastewater using palm kernel shell-derived biochar, Appl. Sci. 10 (2020). https://doi.org/10.3390/app10072251.

[30] S. Varala, B. Dharanija, B. Satyavathi, V.V.B. Rao, R. Parthasarathy, New biosorbent based on deoiled karanja seed cake in biosorption studies of Zr (IV): optimization using Box–Behnken method in response surface methodology with desirability approach, Chem. Eng. J. 302 (2016) 786–800.

[31] S.R.M. Moghddam, A. Ahad, M. Aqil, S.S. Imam, Y. Sultana, Formulation and optimization of niosomes for topical diacerein delivery using 3-factor, 3-level Box-Behnken design for the management of psoriasis, Mater. Sci. Eng. C. 69 (2016) 789–797.